Non-thermal effects of terahertz radiation on gene expression in mouse stem cells

Boian S. Alexandrov,[1] Kim Ø. Rasmussen,[1,6] Alan R. Bishop,[1] Anny Usheva,[3] Ludmil B. Alexandrov,[2] Shou Chong,[3] Yossi Dagon,[3] Layla G. Booshehri,[4] Charles H. Mielke,[4] M. Lisa Phipps,[5] Jennifer S. Martinez,[5] Hou-Tong Chen,[5] and George Rodriguez[5,7]

[1]Theoretical Division, Los Alamos National Laboratory, Los Alamos, NM 87545, USA
[2]Wellcome Trust Sanger Institute, Cambridge, CB10 1SA, UK
[3]Harvard Medical School, Beth Israel Deaconess Medical Center, Department of Medicine, Boston, MA 02215, USA
[4]Materials Physics and Applications Division - NHMFL, Los Alamos National Laboratory, Los Alamos, NM 87545 USA
[5]Center for Integrated Nanotechnologies, Los Alamos National Laboratory, NM 87545, USA
[6]kor@lanl.gov
[7]rodrigeo@lanl.gov

Abstract: In recent years, terahertz radiation sources are increasingly being exploited in military and civil applications. However, only a few studies have so far been conducted to examine the biological effects associated with terahertz radiation. In this study, we evaluated the cellular response of mesenchymal mouse stem cells exposed to THz radiation. We apply low-power radiation from both a pulsed broad-band (centered at 10 THz) source and from a CW laser (2.52 THz) source. Modeling, empirical characterization, and monitoring techniques were applied to minimize the impact of radiation-induced increases in temperature. qRT-PCR was used to evaluate changes in the transcriptional activity of selected hyperthermic genes. We found that temperature increases were minimal, and that the differential expression of the investigated heat shock proteins (HSP105, HSP90, and CPR) was unaffected, while the expression of certain other genes (Adiponectin, GLUT4, and PPARG) showed clear effects of the THz irradiation after prolonged, broad-band exposure.

OCIS codes: (170.1420) Biology; (170.1530) Cell analysis; (170.7160) Ultrafast technology.

References and links

1. R. M. Woodward, B. E. Cole, V. P. Wallace, R. J. Pye, D. D. Arnone, E. H. Linfield, and M. Pepper, "Terahertz pulse imaging in reflection geometry of human skin cancer and skin tissue," Phys. Med. Biol. **47**(21), 3853–3863 (2002).
2. S. J. Oh, J. Kang, I. Maeng, J. S. Suh, Y. M. Huh, S. Haam, and J. H. Son, "Nanoparticle-enabled terahertz imaging for cancer diagnosis," Opt. Express **17**(5), 3469–3475 (2009).
3. V. P. Wallace, A. J. Fitzgerald, S. Shankar, N. Flanagan, R. Pye, J. Cluff, and D. D. Arnone, "Terahertz pulsed imaging of basal cell carcinoma ex vivo and in vivo," Br. J. Dermatol. **151**(2), 424–432 (2004).
4. R. Appleby and H. B. Wallace, "Standoff detection of weapons and contraband in the 100 GHz to 1 THz region," IEEE Trans. Antenn. Propag. **55**(11), 2944–2956 (2007).
5. J. F. Federici, B. Schulkin, F. Huang, D. Gary, R. Barat, F. Oliveira, and D. Zimdars, "THz imaging and sensing for security applications: explosives, weapons and drugs," Semicond. Sci. Technol. **20**(7), S266–S280 (2005).
6. D. Zimdars and J. S. White, "Terahertz reflection imaging for package and personnel inspection," Proc. SPIE **5411**, 78–83 (2004).
7. L. Thrane, R. H. Jacobsen, P. Uhd Jepsen, and S. R. Keiding, "THz reflection spectroscopy of liquid water," Chem. Phys. Lett. **240**(4), 330–333 (1995).
8. P. U. Jepsen, U. Møller, and H. Merbold, "Investigation of aqueous alcohol and sugar solutions with reflection terahertz time-domain spectroscopy," Opt. Express **15**(22), 14717–14737 (2007).
9. G. J. Wilmink and J. E. Grundt, "Invited review article: current state of research on biological effects of terahertz radiation," J. Infrared Millimeter Terahertz Waves (2011), http://dx.doi.org/10.1007/s10762-011-9794-5.
10. THz-BRIDGE Project web-page (2004), http://www.frascati.enea.it/THz-BRIDGE/.
11. T. T. L. Kristensen, W. Withayachumnankul, P. U. Jepsen, and D. Abbott, "Modeling terahertz heating effects on water," Opt. Express **18**(5), 4727–4739 (2010).

#149901 - $15.00 USD Received 27 Jun 2011; revised 11 Aug 2011; accepted 17 Aug 2011; published 23 Aug 2011

12. G. J. Wilmink, B. D. Rivest, C. C. Roth, B. L. Ibey, J. A. Payne, L. X. Cundin, J. E. Grundt, X. Peralta, D. G. Mixon, and W. P. Roach, "In vitro investigation of the biological effects associated with human dermal fibroblasts exposed to 2.52 THz radiation," Lasers Surg. Med. **43**(2), 152–163 (2011).
13. G. J. Wilmink, B. L. Ibey, C. L. Roth, R. L. Vincelette, B. D. Rivest, C. B. Horn, J. Bernhard, D. Roberson, and W. P. Roach, "Determination of death thresholds and identification of terahertz (THz)-specific gene expression signatures," Proc. SPIE **7562**, 75620K, 75620K-8 (2010).
14. A. Korenstein-Ilan, A. Barbul, P. Hasin, A. Eliran, A. Gover, and R. Korenstein, "Terahertz radiation increases genomic instability in human lymphocytes," Radiat. Res. **170**(2), 224–234 (2008).
15. J. S. Olshevskaya, A. S. Ratushnyak, and A. K. Petrov, A.S. Kozlov AS, T.A. Zapara, "Effect of terahertz electromagnetic waves on neurons systems," in *IEEE Region 8 International Conference on Computational Technologies in Electrical and Electronics Engineering, 2008. SIBIRCON 2008* (IEEE, New York 2008), pp. 210–211.
16. R. Shiurba, T. Hirabayashi, M. Masuda, A. Kawamura, Y. Komoike, W. Klitz, K. Kinowaki, T. Funatsu, S. Kondo, S. Kiyokawa, T. Sugai, K. Kawamura, H. Namiki, and T. Higashinakagawa, "Cellular responses of the ciliate, Tetrahymena thermophila, to far infrared irradiation," Photochem. Photobiol. Sci. **5**(9), 799–807 (2006).
17. H. Fröhlich, "The extraordinary dielectric properties of biological materials and the action of enzymes," Proc. Natl. Acad. Sci. U.S.A. **72**(11), 4211–4215 (1975).
18. Y. Feng, R. D. Beger, X. Hua, and E. W. Prohofsky, "Breathing modes near a junction of DNA double helices," Phys. Rev. A **40**(8), 4612–4619 (1989).
19. M. Blank and R. Goodman, "Do electromagnetic fields interact directly with DNA?" Bioelectromagnetics **18**(2), 111–115 (1997).
20. H. Urabe, M. Kato, Y. Tominaga, and K. Kajiwara, "Counterion dependence of water of hydration in DNA gel," J. Chem. Phys. **92**(1), 768–774 (1990).
21. B. M. Fischer, M. Walther, and P. Uhd Jepsen, "Far-infrared vibrational modes of DNA components studied by terahertz time-domain spectroscopy," Phys. Med. Biol. **47**(21), 3807–3814 (2002).
22. O. P. Cherkasova, V. I. Fedorov, E. F. Nemova, and A. S. Pogodin, "Influence of terahertz laser radiation on the spectral characteristics and functional properties of albumin," Opt. Spectrosc. **107**(4), 534–537 (2009).
23. W. F. Edwards, D. D. Young, and A. Deiters, "The effect of microwave irradiation on DNA hybridization," Org. Biomol. Chem. **7**(12), 2506–2508 (2009).
24. G. N. Kulipanov, N. G. Gavrilov, B. A. Knyazev, E. I. Kolobanov, V. V. Kotenkov, V. V. Kubarev, A. N. Matveenko, L. E. Medvedev, S. V. Miginsky, L. A. Mironenko, V. K. Ovchar, V. M. Popik, T. V. Salikova, M. A. Scheglov, S. S. Serednyakov, O. A. Shevchenko, A. N. Skrinsky, V. G. Tcheskidov, and N. A. Vinokurov, "Research highlights from the Novosibirsk 400 W average power THz FEL," Terahertz Sci. Technol. **1**(2), 107–125 (2008).
25. S. P. Mickan, A. Menikh, H. Liu, C. A. Mannella, R. MacColl, D. Abbott, J. Munch, and X.-C. Zhang, "Label-free bioaffinity detection using terahertz technology," Phys. Med. Biol. **47**(21), 3789–3795 (2002).
26. P. Haring Bolivar, M. Brucherseifer, M. Nagel, H. Kurz, A. Bosserhoff, and R. Büttner, "Label-free probing of genes by time-domain terahertz sensing," Phys. Med. Biol. **47**(21), 3815–3821 (2002).
27. B. S. Alexandrov, V. Gelev, A. R. Bishop, A. Usheva, and K. Ø. Rasmussen, "DNA breathing dynamics in the presence of a terahertz field," Phys. Lett. A **374**(10), 1214–1217 (2010).
28. P. Maniadis, B. S. Alexandrov, A. R. Bishop, and K. Ø. Rasmussen, "Feigenbaum cascade of discrete breathers in a model of DNA," Phys. Rev. E Stat. Nonlin. Soft Matter Phys. **83**(1), 011904 (2011).
29. J. Bock, Y. Fukuyo, S. Kang, M. L. Phipps, L. B. Alexandrov, K. Ø. Rasmussen, A. R. Bishop, E. D. Rosen, J. S. Martinez, H.-T. Chen, G. Rodriguez, B. S. Alexandrov, and A. Usheva, "Mammalian stem cells reprogramming in response to terahertz radiation," PLoS ONE **5**(12), e15806 (2010).
30. K. Y. Kim, A. J. Taylor, J. H. Glownia, and G. Rodriguez, "Coherent control of terahertz supercontinuum generation in ultrafast laser–gas interactions," Nat. Photonics **2**(10), 605–609 (2008).
31. G. Rodriguez and G. L. Dakovski, "Scaling behavior of ultrafast two-color terahertz generation in plasma gas targets: energy and pressure dependence," Opt. Express **18**(14), 15130–15143 (2010).
32. A. S. Whitehead, K. Zahedi, M. Rits, R. F. Mortensen, and J. M. Lelias, "Mouse C-reactive protein. Generation of cDNA clones, structural analysis, and induction of mRNA during inflammation," Biochem. J. **266**(1), 283–290 (1990).
33. B. S. Alexandrov, V. Gelev, S. W. Yoo, A. R. Bishop, K. Ø. Rasmussen, and A. Usheva, "Toward a detailed description of the thermally induced dynamics of the core promoter," PLOS Comput. Biol. **5**(3), e1000313 (2009).
34. B. S. Alexandrov, V. Gelev, S. W. Yoo, L. B. Alexandrov, Y. Fukuyo, A. R. Bishop, K. Ø. Rasmussen, and A. Usheva, "DNA dynamics play a role as a basal transcription factor in the positioning and regulation of gene transcription initiation," Nucleic Acids Res. **38**(6), 1790–1795 (2010).

1. Introduction

Terahertz (THz) technologies are emerging with many promising medical, military, security, and research applications, e.g., detection of cancer [1–3], airport security systems [4,5], shipment inspection [6], and in spectroscopy [7,8]. Despite this emerging ubiquity of THz applications, relatively little is known about the effect of THz radiation on biological systems.

#149901 - $15.00 USD Received 27 Jun 2011; revised 11 Aug 2011; accepted 17 Aug 2011; published 23 Aug 2011

A recent comprehensive review of THz radiation effects on biological systems is given in Ref. [9]; so we will limit ourselves to discuss the studies most pertinent to our work.

Most previous bio-related studies were conducted under the purview of a single international project—the "THz-BRIDGE" project [10]. This project was aimed at examining the mechanisms governing THz interactions with cells and biomolecules to assess the possible genotoxicity of THz radiation. Most studies associated with this project, found that THz-induced bioeffects were mediated primarily by thermal mechanisms. This finding is not unexpected because water is the solvent for all biological entities and THz radiation is strongly absorbed by water [11]. Some studies of the THz-BRIDGE project reported potential genotoxic and epigenetic effects on human lymphocytes and changes in the membrane permeability of liposomes, but were unable to clarify the exact mechanisms (thermal or non-thermal) behind these effects.

Recently, in a careful study human cells were exposed (for 1-40 min.) to continuous-wave (CW) THz radiation (2.52 THz, and 227 mW/cm^2) in order to investigate genotoxic and cell-death effects [12]. Flow cytometric and MTT analyses were performed on the THz-exposed Jurkat cells, in order to investigate early apoptosis, necrosis, and total death. It was found that the vast majority of cells exposed to this kind of THz radiation for more than 20 minutes appear to be dying via both apoptotic and necrotic pathways. In the same study, the expression of genes, selected from cellular stress response (apoptosis, metabolism, proteolysis, chaperone, redox regulation, and DNA repair) pathways, was monitored. The conclusions were that primary genes affected by THz radiation are inflammatory cytokines. In a follow-on study [13], human dermal fibroblasts were exposed to CW THz radiation (2.52THz, and 84.8 mW/cm^2) for up to 80 minutes. The temperature of the cell cultures was shown to increase more than 3°C as a result of the exposure. Focusing mainly on cell viability and damage mechanisms this investigation found that 90% of the THz-exposed cells survived these conditions, while exhibiting minor increases in the expression of heat shock proteins, which in this study were considered to be DNA damage markers. Importantly, a similar increase in the expression of the same heat shock proteins was observed when the cells where simply exposed to a 3°C hyperthermic shock above physiological temperature. This study therefore concludes that the primary effect of THz exposure is hyperthermal.

However, the above conclusions cannot explain the experimental data from other recent studies conducted at strictly controlled thermal conditions that also demonstrate a THz-related effect on cellular cultures. For example it was confirmed that a very weak CW THz field (0.031 mW/cm^2) may cause genomic instability in human lymphocytes [14] after extended (more than 6 hours) exposure. Independently, it was reported that neurons briefly exposed *in vitro* to powerful THz radiation develop infringements on the morphology of the cellular membranes and intracellular structures [15]. Changes in the gene expression of low eukaryotes have also been documented after prolonged exposure (72 hours) to very low-power, non-coherent, and broad-spectrum THz radiation centered at ~30 THz [16]. All these experiments were conducted under controlled thermal conditions, and it was argued that the temperature is unrelated to the observed effects.

Motivated by the fact that the energy scale of THz radiation is within the range of hydrogen bonds, van der Waals interactions, and charge-transfer reactions, it has long been thought that this non-ionizing electromagnetic field, through *nonlinear resonance mechanisms*, may have a significant effect on cells and biomolecules [17–19]. Consistent with such effects, it has been experimentally demonstrated that THz radiation interacts primarily with the hydrogen bonds [20,21] of the biomolecules and can cause low-frequency intramolecular vibrations that result in conformational changes in proteins [22]. Recently, it was shown that high power, low-frequency (2.45 GHz) irradiation can denature short DNA oligos, well below their thermal melting temperature (between –20°C and 20°C) [23]. This experiment demonstrated that powerful electromagnetic irradiation can result in DNA melting via pathways that are different from thermal effects. Independently, it was shown that high-power THz irradiation (2.3 THz) can also destroy double-stranded DNA hybridization, disrupting the hydrogen bonds between the two complementary strands of the target DNA

#149901 - $15.00 USD Received 27 Jun 2011; revised 11 Aug 2011; accepted 17 Aug 2011; published 23 Aug 2011

oligomers, in the absence of bulk water [24]. The authors suggested that the mechanism of DNA dehybridization occurs by exciting deformational vibrations in the intermolecular hydrogen bonds - O-H...N and N-H...N. The last two experiments also confirmed that the observed dehybridization did not cause any additional damage or destruction of the resulting (melted or "ablated") single stranded DNA and did not affect covalent bonds, which suggests interactions only between THz and DNA's hydrogen bonds.

Taken together, the above studies suggest that THz radiation can interact with biomolecules and cells through non-thermal mechanisms and thus hold the potential to change cellular function in a non-destructive fashion.

It is clear that the non-thermal mechanisms by which the non-ionizing THz radiation influences biological functions must be fundamentally different from those at play when high-energy (UV, X-ray, gamma, etc.) radiation interacts and damages bio-matter. While the mechanism by which THz radiation couples to, and subsequently affects, the function of biomolecules (e.g., DNA and proteins), remains unclear, there is ample evidence that exposure to THz radiation can affect the intramolecular vibrations and hence dynamically induce new conformational states [21,22,25,26]. The coupling mechanism is believed to be due to the fact that a THz field oscillates on the picosecond time scale, corresponding to the phonon frequencies of double-stranded DNA (dsDNA). In fact theoretical models have been developed [27,28] that suggest that THz radiation may couple directly to biomolecules via nonlinear resonance mechanisms to induce coherent excitations in the form of localized openings (bubbles) of the DNA strands. The described nonlinear resonance mechanism is active even for small amplitudes [28] of the THz field, but it is probabilistic and therefore requires extended exposure. The conformations generated through this mechanism can subsequently interfere with transcription and protein-binding processes, and thereby induce changes in cellular gene expression of the active genes.

In this light, the question of whether mammalian cells exposed to THz radiation exhibit specific cellular and/or molecular effects, unrelated to the temperature changes, is important. As indicated theoretically [27,28] such effects need not be directly related to protein and/or DNA damage but they may well be significantly subtler and only cause functional changes whose effects can be accumulated over time.

To investigate these issues, we conducted THz exposures of mesenchymal mouse stem cell cultures using a unique pulsed broad-band (1THz–30 THz) plasma gas radiation source, as well as an optically pumped molecular gas CW THz laser source (2.52 THz). The irradiations were performed at biologically-low temperatures (26–27°C), and at low THz power average densities (~1–3 mW/cm^2), in order to minimize thermal effects on the gene activity.

This study builds off of our earlier work [29] that reported differential response of genes (connected with cell differentiation) to a pulsed broad-band THz irradiation. In order to emphasize that the observed effects in the differential expression are not of thermal origin, we report here response of hyperthermic genes (i.e. genes that usually respond to temperature increases in the cell) to both pulsed and CW THz radiation. To analyze the possible changes in the temperature in our experiments we applied simulations and experimental measurements, including modeling approaches, thermo-sensors, and infrared cameras. To examine the eventual thermal effect locally, i.e. in the cells, we quantify the THz-induced transcriptional activation of hyperthermic genes using qRT-PCR, and compare their expression levels with previously reported differentially expressed genes.

2. Materials and methods

2.1. Mouse stem cell culture

Mouse mesenchymal stem cells (MSCs) (ScienCell Research Laboratories, CA 92011, Catalog Number M7500) were cultured on tissue-culture treated plastic T-75 flasks (Corning). Once the cells reached 80-90% confluence, the cells were sub-cultured in supplemented medium (95% α-MEM, 5% FBS, and antibiotics) for THz irradiation treatment. Roziglitazone

#149901 - $15.00 USD Received 27 Jun 2011; revised 11 Aug 2011; accepted 17 Aug 2011; published 23 Aug 2011

(1 μM), insulin (5 μg/ml), 3-Isobutyl-1-methylxanthine (100 μM), and dexamethasone (1 μM) were added to the medium 110 hours prior to irradiation and again 48 hours prior to irradiation.

2.2. Terahertz sources and irradiation

1. Through the frequency mixing of ultrafast fundamental and second-harmonic laser fields, a directional electrical current in pressurized atomic gases can be generated. In the case of ultrafast lasers (<100 fs) this technique is capable of producing electromagnetic radiation at THz frequencies [30]. We use a recently developed coherent-control scheme optimizing for such type of THz generation in gases, yielding a new source of high-energy (~1 μJ, pulse width ~35 fs, i.e., high peak power per pulse ~30 MW), broadband THz radiation (centered at ~10 THz, Fig. 1) at a high repetition rate of 1 kHz.

2. In addition, we used a far-IR optically pumped molecular gas CW THz laser source (Edinburgh Instruments FIRL 100). All experiments with this laser were conducted using methanol (CH_3OH) producing a beam at frequency 2.52 THz (λ = 118.8 μm). The beam profile was very close to Gaussian since it is composed of more than 90% TEM_{00} mode, with an aperture of ~12mm. The power was determined with a calibrated Scientech (model #AC2500H) laser powermeter.

For the broadband THz source, 35 fs THz pulses are generated in a two-color laser photoionization gas plasma mixing scheme [31]. The laser system consists of an 800 nm 40 fs Ti:sapphire oscillator, regenerative amplifier, and single pass amplifier. Output pulses from the oscillator are amplified to 6 mJ per pulse at a pulse repetition frequency of 1 kHz. The laser beam is then directed to a pure argon filled gas cell (600 Torr) for THz generation. The gas cell also contains a type I second harmonic nonlinear crystal (beta-barium borate - BBO) for generation of the second color 400 nm beam that propagates collinearly with the fundamental (800 nm) beam for the two-color THz generation process. Focusing (f = 12.5 cm) of the two-color laser beams into the gas cell rapidly photoionizes the argon gas and produces a plasma spark in which fully coherent ultrafast 35 fs THz pulses are generated via a complex nonlinear plasma current mixing mechanism [30,31]. The residual optical beams that exit the THz generation interaction region are then spectrally blocked with a 1-inch diameter 600 μm thick high resistivity silicon filter that also serves as the gas cell exit window. The silicon filter is an excellent THz transmission filter and transmits the entire spectrum of the THz pulse. Fresnel losses limit the transmission efficiency of the silicon filter to approximately 50%. Optical to THz conversion efficiencies with this scheme are approximately $2x10^{-4}$ with single pulse THz energies approaching 1 μJ at our detector after the silicon filter. Absolute power (energy) measurements are made using a high sensitivity 5-mm diameter $LiTaO_3$ pyroelectric detector (Model SPH-45-OB, Spectrum Detector Inc.). This detector is windowless and is coated with an energy absorbing black coating layer that is well suited for sensitivity across the entire band of our broadband THz source. The relative spectral response of the detector is flat to within a few percent across the entire range: visible (λ = 400 nm) to THz frequencies (λ = 300 μm). The responsivity of the detector is $R_v = 4.5x10^4$ V/W at a pulse repetition frequency of 5 Hz. Principal drawback of the detector is its relatively slow thermal response time making the detector approximately 100 times less responsive at 1 kHz (the repetition rate of our laser and THz source). THz irradiance measurements are made by recording the measured detector voltage and dividing by the detector responsivity and area. Crosscheck of our measurements are done by calibrated measurements at 800 nm using the same pyroelectric detector, and a second silicon based photodetector, to compare with the known power from an attenuated pickoff beam from our laser. For irradiating the samples, the THz beam is allowed to exit the gas cell and naturally diverge (after the initial f = 12.5 cm two-color optical beam focus) to a beam diameter that has approximately the cross-sectional area size of the culture petri dish (4 cm diameter). The measured irradiance of the center of

#149901 - $15.00 USD Received 27 Jun 2011; revised 11 Aug 2011; accepted 17 Aug 2011; published 23 Aug 2011

the beam THz beam after transmission through an empty culture plate was 1.2 mW/cm^2. Due to a Gaussian shaped THz beam, irradiance level near the edge of the plate is 0.25 mW/cm^2.

For the THz temporal interferograms and power spectrum measurements we built an all reflective scanning leg Michelson interferometer [31]. After the THz generation gas cell, a 90 degree off-axis parabolic gold mirror was to collect and collimate the THz beam before directing the THz beam to the interferometer. The interferometer consists of all reflective 2 inch diameter gold flat mirrors using a 2 μm gold coated IR/FIR mylar pellicle 50/50 main beamsplitter to split (and recombine) the THz beam into each arm of the interferometer. Spatially integrated detection of the resulting interference beam is done by collecting the entire beam with a second 90 degree off-axis parabolic gold mirror focused to a point on the previously described pyroelectric detector. Measurements of the THz spectrum were done in vacuum to eliminate possible effects of atmospheric water absorption [31]. Measurement of the terahertz spectrum is done by first recording a time-domain intensity autocorrelation interferogram. By scanning one arm of the Michelson interferometer as an optical delay line using

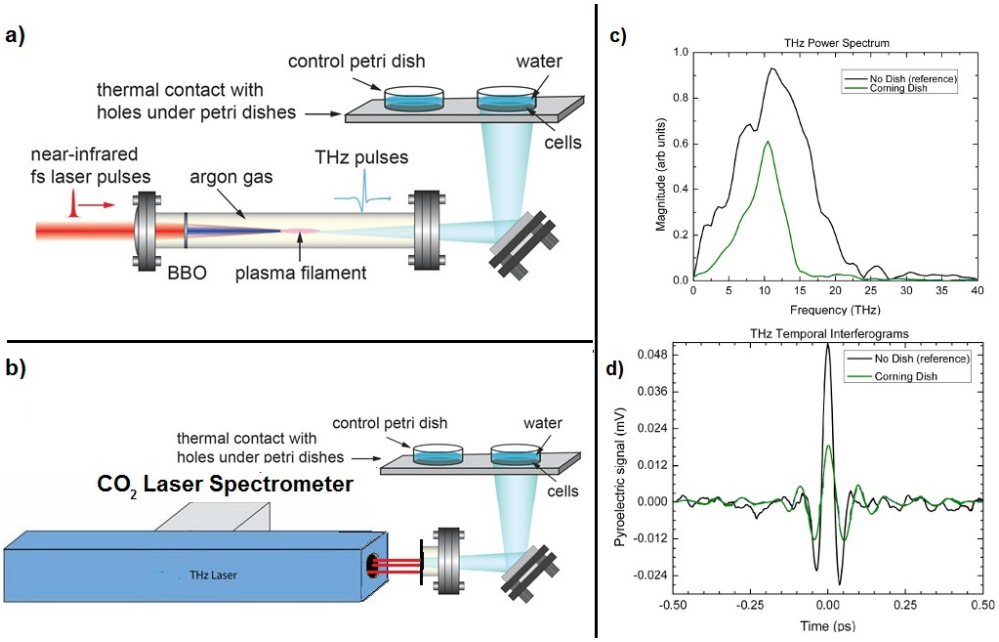

Fig. 1. Schematic representation of the experimental setups: a) Pulsed broad–band source; b) CW laser source; c) Power spectrum of the broad-band source, with and without petri dish; d) The temporal interferograms of the broad-band source, with and without petri dish.

computer controlled motorized linear translation stage, the pyroelectric detector detects a voltage signal generated by the temporal autocorrelation of the THz pulses in each arm of the interferometer. Data is readout using a lock-in amplifier as a function of positional delay resulting in a time-domain intensity interferogram. A numerical Fourier transform is performed on the temporal interferogram data to extract the terahertz power spectrum. Figure 1 shows the results of the c) retrieved spectra from the d) temporal intensity autocorrelation interferograms for cases with and without an empty petri dish. These measurements clearly show the reduction in THz bandwidth due to the material losses arising from the dish, especially above 15 THz.

2.3. Experimental setup and thermal considerations

Cells were irradiated in parafilm-sealed tissue culture plates (diameter 4 cm) in the presence of culture medium. The ambient temperature was held constant at the relatively low

#149901 - $15.00 USD Received 27 Jun 2011; revised 11 Aug 2011; accepted 17 Aug 2011; published 23 Aug 2011

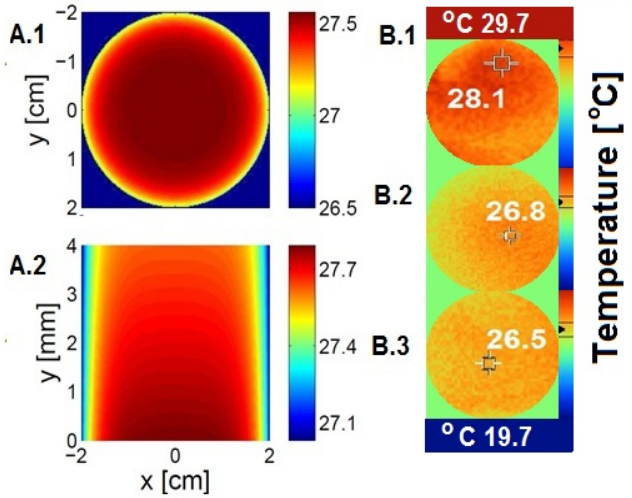

Fig. 2. Calculated thermal profiles: A.1 shows the top view of the steady state thermal profile in the presence of irradiation from the laser source. A.2 shows the side view of the steady state thermal profile in the presence of irradiation from the laser source. Cells are positioned at the dish bottom (z = 0). B). Measured (by IR detector) thermal profiles: B.1 represent a top view snapshot of the petri dish after 2 hours of irradiation from the CW laser source. B.2 represent top view snapshot after 2 hours of irradiation from the broad-band source. B.3 represent top view snapshot of non-irradiated (control) petri dish. All the cell cultures were thermoequilibrated slightly above the ambient room temperature (panel B.3).

temperature of 26.5°C ± 0.2°C in order to avoid thermal stress due to the slight temperature increase caused by the THz exposure. Cells were irradiated for 2, and 9 hours in two replicates (the experimental setups of the broad-band source, and for single-frequency laser source are shown in Figs. 1a and 1b). Controls consisted of identical cell plates and conditions but were not irradiated. In the case of the pulsed broad-band source cell viability and morphology were visually monitored by light microscopy, 100 x magnifications (Nikon). The broad-band spectrum and temporal interferogram, with and without a petri dish, are shown at Figs. 1c and 1d. During irradiation by the laser source light microscopy was not applied. Our use of large-area (12.56 cm^2) plates results in relative low average power densities: ~1 mW/cm^2 for the pulsed broad-band source, and ~3 mW/cm^2 for the CW laser source. These power densities account for the loss incurred by penetrating the dish bottom (see Fig. 1a, for the broad-band source), and thus represent the densities at the cell/media surface. The temperature of the cells during irradiation was monitored using both an IR camera (FLUKE Ti10, thermal sensitivity < 0.2°C at 30°C), and thermo-sensors glued to the outside of the petri dish lids. In order to anticipate the thermal effects involved in the experiments we adapted the theoretical formalism developed in Ref. [11] for solving the heat equation relevant to our particular situation. In contrast to Ref. [11], we used convective boundary conditions at the air-media (top) interface using a heat transfer coefficient equal to h = 30 $Wm^{-2}°C^{-1}$ [12], while assuming negligible heat loss to the dish (bottom and sides) consistent with what was observed by the external thermo-sensors. The calculated steady state temperature profiles in the case of the laser source are shown in Fig. 2. Figure 2 A.1 shows that a temperature increase of about 1.5°C is anticipated at the bottom of the dish (location of cells) and about 1°C at the top of the dish (location of IR camera). These estimates are in agreement with the observed values as shown in Fig. 2 A.2.

2.4. Isolation of RNA and qRT-PCR

Cellular RNA was extracted using the RNeasy Mini kit (Qiagen) following the manufacturer's instructions. For cellular qRT–PCR, 500 ng total RNA was reverse transcribed using a reverse transcription kit (Clontech, Advantage RT-for-PCR) with random-oligo primers; qRT-PCR reactions were assembled in triplicates with 1 μM gene specific primers and 5 μl Applied

#149901 - $15.00 USD Received 27 Jun 2011; revised 11 Aug 2011; accepted 17 Aug 2011; published 23 Aug 2011

Biosystems SYBR Green PCR Master Mix in 10 µl reactions. qPCR was executed in a 384-well block Applied Biosystem 7900-HT Real-time PCR machine. Gene specific primers were selected (PRIMER BLAST, NIH). TBP (TATA box binding protein) was used as internal control. The sequences of the primers are: Hsp90 (Heat shock protein90) - GTGCGAGTCGGACTTGG and TGAAAG GCAAAGGTCTCCAC; Hsp105 (Heat shock protein105) - ACATAAGGCTGA GCGATTGG, CGCAATGTAGCAGCTCTGT; CRP(C reactive protein) - CCAGGACTCCTTGTCCTTG, TCATGATCAGAAGGCACCAG. The comparative CT method (Applied Biosystems) was used to analyze the data resulting from the qRT-PCR experiments.

3. Results

3.1. Morphological changes in mouse stem cells after THz irradiation

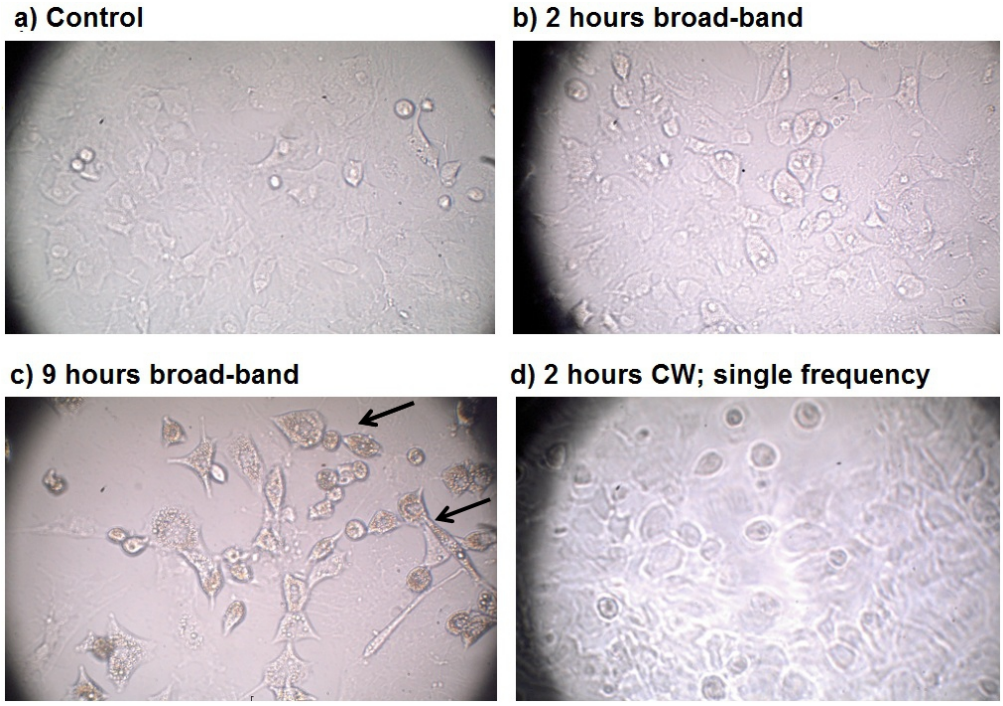

Fig. 3. Light microscopy image: a) Control cultures; Mouse stem cells after: 2 hours - b) and 9 hours - c), of pulsed broad-band irradiation; d) Mouse stem cells after 2 hours of irradiation from the CW laser source. The arrows in c) indicate cells with an elevated number of lipid droplets inclusions.

Figure 3 shows typical light microscopy images of the control sample, and the exposed samples after 2 and 9 hours of pulsed broad-band exposure as well as after 2 hours of CW exposure. No cell death was visually observed, but the cell viability was not quantified in detail. No effects on the cell membranes were visually discernable. No lipid inclusions were observed in the control samples or in the samples that were exposed to 2 hours of CW irradiation. However, lipid droplet-like inclusions were observed in the cellular cytoplasm after 2 and 9 hours of broad-band exposure. Significantly, fewer cells were observed to contain such inclusions in the cells exposed only for 2 hours as well as in the control MSC cultures. This clearly suggests that the morphological changes observed in the MSC cytoplasm are dependent of the exposure duration and frequency.

3.2. Effect of THz irradiation on the expression of heat shock proteins

It has previously been argued [13] that an effect on gene expression resulting from THz irradiation would most likely be related only to thermal stress associated with the irradiation.

#149901 - $15.00 USD Received 27 Jun 2011; revised 11 Aug 2011; accepted 17 Aug 2011; published 23 Aug 2011

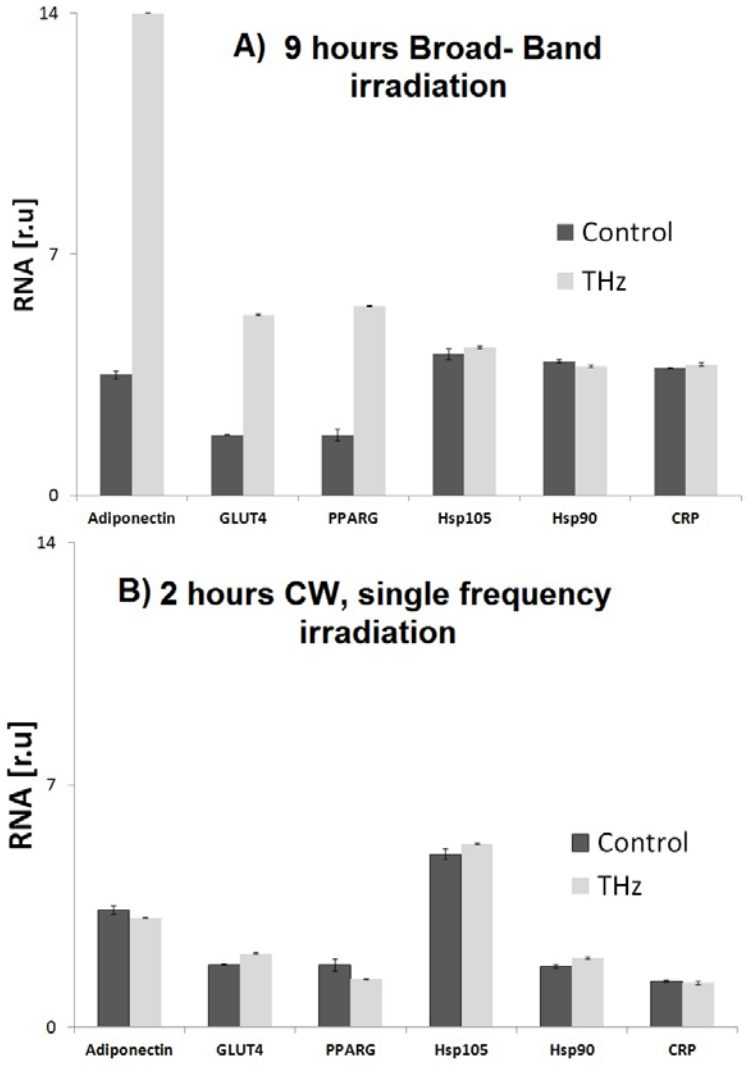

Fig. 4. A) Comparison between the differential gene expression of the heat shock proteins Hsp105, Hsp90, and the C-reactive protein (CRP) and previously reported [29] up-regulated genes in response to 9 hours of exposure from the broad-band source. B) Differential gene expression of the heat shock proteins Hsp105, Hsp90, and the C-reactive protein (CRP) together with the differential expression of GLUT4, Adiponectin and PPARG in response to 2 hours of exposure from the CW source. Expression levels are normalized to the expression level of the TBP gene, as in Ref. [29]. The identities of the genes are given below the X-axes. Light grey bars: THz exposed cells, Dark grey bars: control cells. The number of specific transcripts is shown on the vertical axis in relative units [r.u.]. The experimental results are consistent between three independent qRT-PCR measurements in duplicates (the standard deviation is shown with errors bars) and in two different sets of irradiation.

genes were down or up-regulated in the same cellular cultures (see Ref. [29]). For comparison we show the differential gene expression response of a few of the strongly up-regulated genes resulting from the pulsed broad-band irradiation as reported in Ref. [29]. The lack of a measurable differential expression of the investigated hyperthermic genes suggests that, even locally, the measured temperature elevation in the cell culture from 26.5°C to 26.8°C (Fig. 3B2), in response to the broad-band THz irradiation is not sufficient to activate the expression of the heat shock proteins, Hsp90, Hsp105, and CRP. Importantly, the presence of down- and up-To analyze for possible THz-related heat effects irradiated mouse stem cells have been

#149901 - $15.00 USD Received 27 Jun 2011; revised 11 Aug 2011; accepted 17 Aug 2011; published 23 Aug 2011

analyzed for expression of the heat shock proteins Hsp90 and Hsp105 as well as the C-reactive protein (CRP) by qRT-PCR. As shown in Fig. 4A, the level of expression of these genes remains nearly unchanged after 9 hours broad-band THz irradiation, while various other regulated genes in the same samples indicates that there is a non-thermal THz-associated mechanism that can change gene expression. In the laser source experiment (2 hour exposure of CW radiation at 2.52 THz), the IR camera showed a slight temperature elevation, viz., from 26.5°C to 28.1°C (Fig. 3B1), and a slightly activated expression of Hsp90 (Fig. 4B). However, the level of the other heat shock and stress response genes Hsp105 and CRP remains nearly constant. In this case, the reaction of Hsp 90 to THz is more likely to be gene specific than temperature related, given that no change in the expression of Hsp 105 was measured. The nearly identical level of Hsp105 expression in both cell cultures (control and irradiated) suggests the absence of heat related response. Moreover, the level of the stress responsive gene CRP that is activated in dying cells [32] remains low in both control and irradiated cells, which suggests the absence of cellular stress response. Also, we observe a lack of differential gene expression in the genes GLUT4, Adiponectin, and PPRAG (Fig. 4B).

4. Discussion

A number of studies have been performed to clarify THz radiation's influence on biological matter and function. A useful summary of these studies has been given in Table 1 of Ref. [13]. It is clear from this summary that the cell types, exposure characteristics (frequency, power, duration, etc.), thermal conditions, as well as endpoint evaluation techniques vary greatly between these studies. While this naturally makes it difficult to draw general conclusions, it is clear that many of the previous studies did not find significant changes in viability, growth or cell morphology. Because of the strong absorption of water at THz frequencies, it is natural to first assume that primary biological effects will arise due to heating, and this is very consistent with observations at high power CW irradiations. It is apparent that thermal effects will mask all other effects in cases where significant heating occurs, particularly if the cell temperatures exceeds 39°C, where specific gene activation occurs irrespective of the cause of the temperature increase. However, in the studies [14–16,29] in which extended exposure was performed *without* causing a significant temperature increase, more subtle effects such as changes in gene expression profiles, genetic instability, and conformational changes were found.

One significant concern surrounding these results is that no comprehensive explanation for how such effects may arise exists. Our suggestion [27,28] is that THz radiation may affect gene expression by perturbing the conformational dynamics of double-stranded DNA. This suggestion is rooted in our prior work [33,34] that establishes a strong relationship between conformational dynamics of double-stranded DNA and cellular function, coupled with the fact that THz photons possess the energy required to influence the dynamics of dsDNA. Given the prior experimental findings and the theoretically suggested mechanism, we designed the experiments described herein to explore the existence of THz related effects on gene expression that can be unambiguously distinguished from thermal effects.

The results of this study shows that mouse mesenchymal stem cells exposed to THz radiation exhibit specific changes in cellular function that are closely related to the gene expression. Our qRT-PCR gene expression survey reveals that some genes in irradiated Mouse stem cell cultures are activated, while other genes are suppressed. The fact that most genes do not respond to the used radiation conditions used here, demonstrates a specific rather than a general response. It is important that these effects where observed under irradiation conditions that caused minimal temperature changes, and in the explicit absence of any discernable response of heat shock and cellular stress genes.

Further investigations involving a large number of genes and variation in THz radiation characteristics and exposure duration are needed to generalize our findings. Also, more direct experimental investigations of THz radiation's ability to induce specific openings of the DNA double-strand are needed in order to fully determine how THz radiation may work through DNA dynamics to influence cellular function.

#149901 - $15.00 USD Received 27 Jun 2011; revised 11 Aug 2011; accepted 17 Aug 2011; published 23 Aug 2011

Acknowledgments

This work was performed, in part, at the Center for Integrated Nanotechnologies, a U.S. Department of Energy, Office of Basic Energy Sciences user facility at Los Alamos National Laboratory (Contract DE-AC52-06NA25396) and Sandia National Laboratories (Contract DE-AC04-94AL85000). Funding from National Institutes of Health (GM073911 to A. U.) is also acknowledged.

#149901 - $15.00 USD Received 27 Jun 2011; revised 11 Aug 2011; accepted 17 Aug 2011; published 23 Aug 2011